

Effects of a non-universal IMF and binary parameter correlations on compact binary mergers

L.M. de Sá, A. Bernardo, R.R.A. Bachega, L.S. Rocha, J.E. Horvath

Instituto de Astronomia, Geofísica e Ciências Atmosféricas
Universidade de São Paulo

lucasmdesa@usp.br



Abstract

Binary population synthesis provides a direct way of studying the effects of different choices of binary evolution models and initial parameter distributions on present-day binary compact merger populations, which can then be compared to empirical properties such as observed merger rates. Samples of zero-age main sequence binaries to be evolved by such codes are typically generated from an universal IMF and simple, uniform, distributions for orbital period P , mass ratio q and eccentricity e . More recently, however, mounting observational evidence has suggested the non-universality of the IMF and the existence of correlations between binary parameters. In this study, we implement a metallicity- and redshift-dependent IMF alongside correlated distributions for P , q and e in order to generate representative populations of binaries at varying redshifts, which are then evolved with the COMPAS code in order to study the variations in merger rates and overall population properties.

Introduction

The beginning of direct gravitational detections by the LIGO, Virgo and now KAGRA observatories has gradually allowed more constraints to be placed on the properties and origins of binary compact mergers (BCMs). One of the most useful tools in this regard have been rapid binary population synthesis (BPS) codes, which can perform the isolated evolution of large samples of binary systems from zero-age main sequence (ZAMS) conditions up to a present day population under a wide set of models.

Most often in BPS, the primary mass (M_1) is taken to be distributed according to a universal IMF and the mass ratio ($q = M_2/M_1 \leq 1$), orbital period ($\log P$) and eccentricity (e) from uniform distributions or fixed values. However, observational evidence has gradually mounted in support of a more complicated picture. The IMF has long been expected to become top-heavy at low metallicities, and suggestions of this behavior have been observed and fitted to an environment-dependent IMF. On the other hand, the q , e and the orbital period (P) have all been shown to inter-correlated and M_1 -dependent. In this work, we have applied both relations in generating ZAMS binary samples to be evolved with the COMPAS BPS code, in order to study the cosmic evolution of BCM properties.

Materials and Methods

Inter-correlated binary parameters

For generating our initial samples, we fully adopt the binary parameter distributions from Moe & Di Stefano (2017); due to the distributions' observational limitations, we are restricted to $M_1 > 0.8 M_\odot$, $q > 0.1$ and $0.2 < \log P < 8$ binaries, which should not significantly affect our results for neutron star (NS) and black hole (BH) binaries. For each M_1 sampled from the IMF described in the next section, we sample $\log P$ according to their companion frequency, $f_{\log P; q \geq 0.1}(M_1)$, fit. Then, given each $M_1, \log P$ pair, we sample q and e from their respective probability distributions, $p_q(M_1, \log P)$ and $p_e(M_1, \log P)$; these are a two-part power law with an excess at $q \geq 0.95$ and a simple power-law, respectively.

IMF

We adopt the integrated galaxy-wide IMF (IGIMF) from Jeřábková et al. (2018). Within the IGIMF theory framework in which this IMF is calculated, stellar formation within a galaxy is considered to take place within embedded clusters (ECLs), individual regions with a given metallicity (Z) and stellar mass (M_{ecl}). The galaxy-wide IMF is then the result of integration over the IMF of all ECLs. By adopting a composition-dependent IMF for the ECLs, the IMF becomes non-universal also for galaxies.

The metallicity-dependent IMF from Marks et al. (2012), a three-part power law, is taken as the stellar IMF (ξ_*) within an ECL; because star formation is constrained by the amount of gas available, this IMF is a distribution over the mass M of stars of the form $\xi_*(M; [\text{Fe}/\text{H}], M_{\text{ecl}})$, with more massive ECLs producing more massive stars. By considering a galaxy as chemically homogeneous, integration over ECLs becomes an integration over M_{ecl} . A power law ECL IMF is adopted as a distribution $\xi_{\text{ecl}}(M_{\text{ecl}}; \text{SFR})$; it is, like the stellar IMF, limited by the total amount of gas in the galaxy, proportional to the SFR. The IGIMF is then

$$\xi(M; \text{SFR}, Z) = \int_0^\infty \xi_*(M; Z, M_{\text{ecl}}) \xi_{\text{ecl}}(M_{\text{ecl}}; \text{SFR}) dM_{\text{ecl}}. \quad (1)$$

SFR

For working with the SFR, we adopt the three empirical relations employed by Chruślińska et al. (2020) in calculating their

star-formation rate density (SFRD) distribution over metallicity (Z) and redshift (z). These redshift-dependent relations describe mean galaxy properties as a function of galaxy stellar mass. We adopt their mass-metallicity (MZR) and mass-SFR (SFMR) relations to tie the two quantities at each redshift, while the sampling of (Z , SFR) pairs is made at each z according to the galaxy stellar mass function (GSMF), a galaxy density distribution which links each (Z , z , SFR) to a correspondent star-forming mass (M_{SFR}). We adopt their intermediary-metallicity fiducial model.

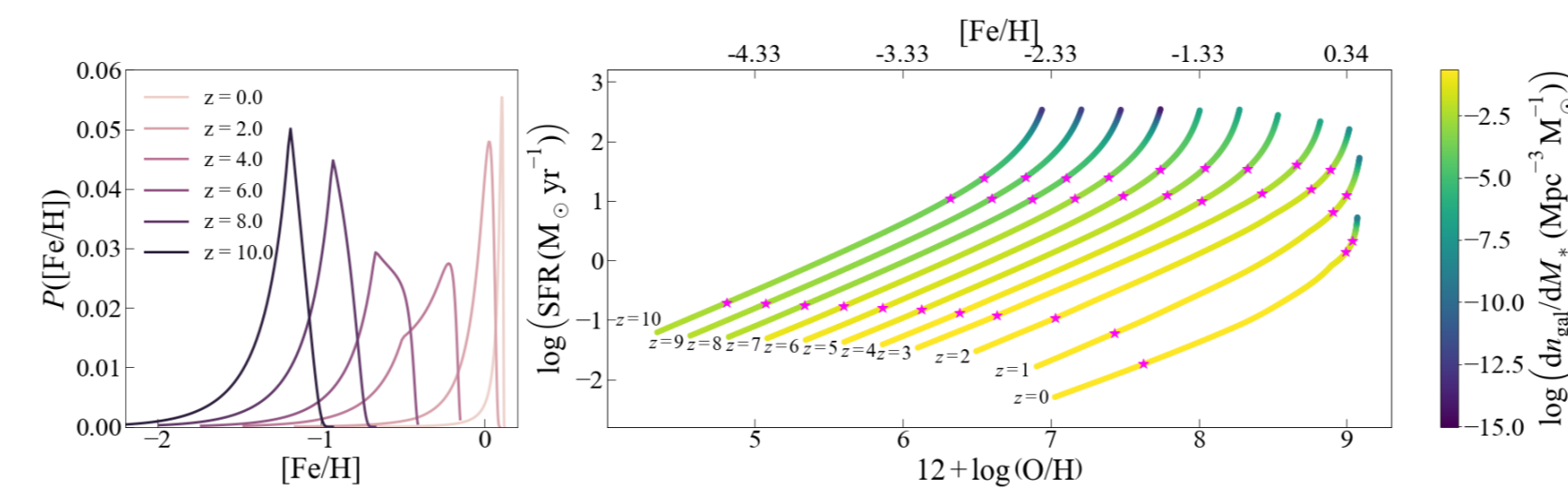


Figure 1: Right: curves representing the resulting metallicity-SFR at different redshifts, colored by the GSMF at each point. Magenta stars show the sampling of three metallicities per redshift according to the GSMF. Left: metallicity distribution per redshift resulting from the MZR, SFMR and GSMF.

By matching the SFR, Z and z in this way, we are able to effectively treat the IGIMF as a $\xi(M; Z, z)$ distribution, allowing us to build samples representative of those conditions today observed at any given redshift z_{ZAMS} .

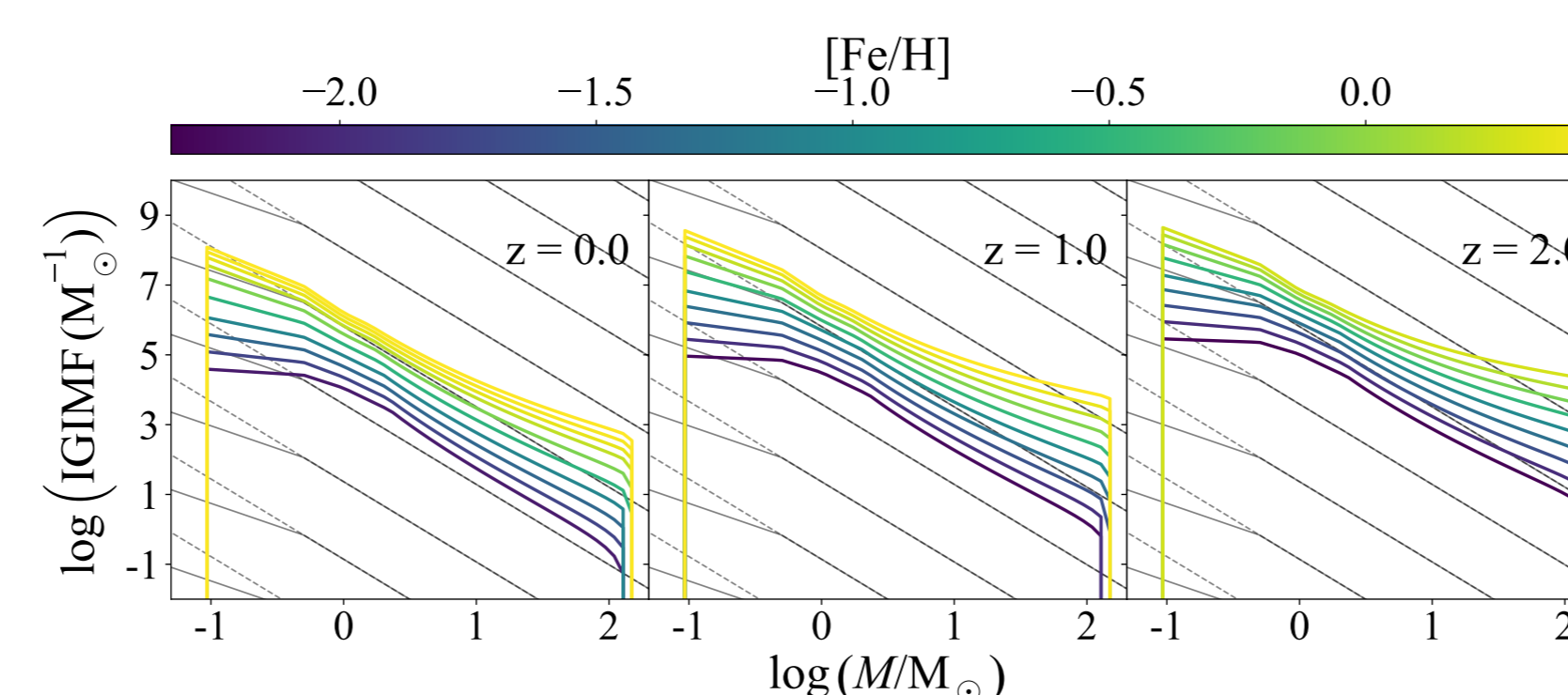


Figure 2: The varying IGIMF for different metallicities at different redshifts. The dark solid line represents the Kroupa universal IMF, and the dashed line the Salpeter IMF, from which Kroupa deviates at low masses.

Results

The results presented here have been derived from 12 samples of $\approx 10^6$ binaries each, for three metallicities sampled by stellar mass density at each $z_{\text{ZAMS}} = 0.5, 1, 2, 3$; they correspond to the magenta stars at the corresponding redshifts in Figure 1. These were then evolved for 13.8 Gyr in COMPAS. While it still left to increase the resolution of our initial sample, it has already been possible to obtain promising behaviors and estimates from this limited set.

In Figure 3, we show the total mass (M_{tot}) distribution for all formed compact binaries separated by type and z_{ZAMS} , as the binary count per M_{tot} bin, per star-forming mass. While all classes show a tendency for more massive systems to have been formed earlier, this is seen to be particularly strong for BHs. Although it is possible that the initial mass range of NS progenitors is not as strongly redshift-dependent as that of BH progenitors, we cannot yet discard the possibility that this is a product of our BNS sample being currently about 10 times smaller than the BBH or BHNS samples.

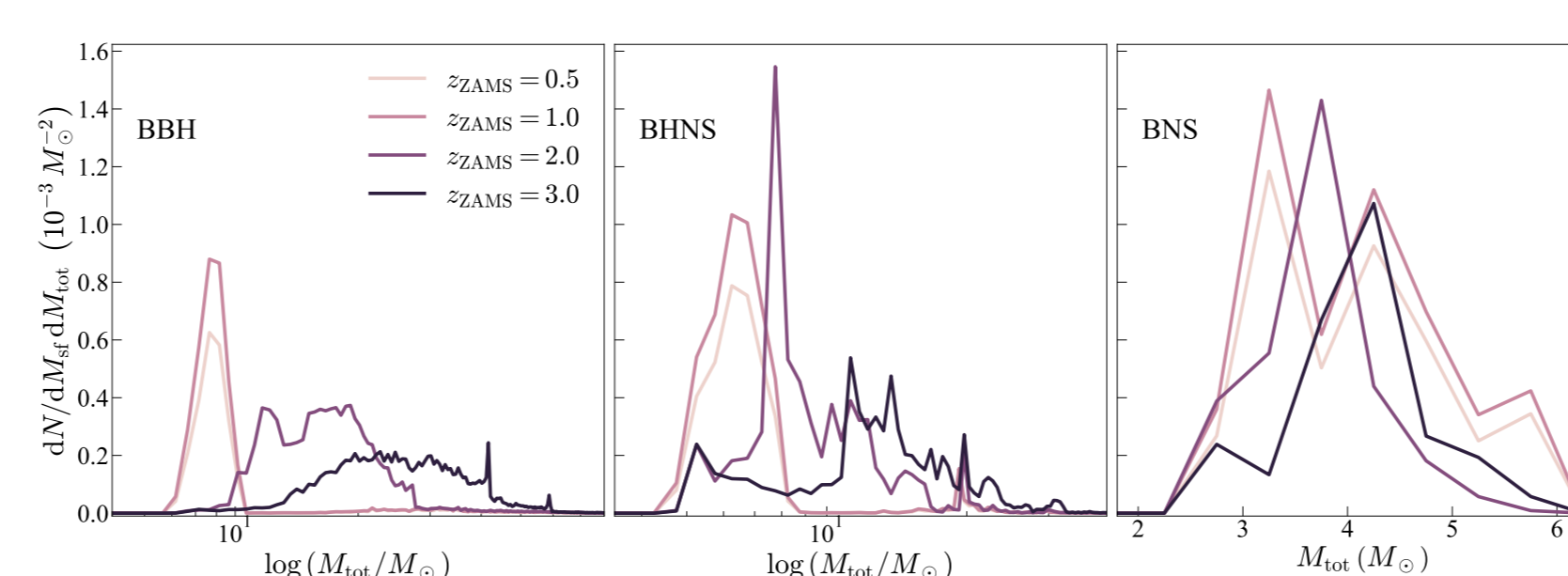


Figure 3: Total mass distributions for all compact binaries separated by class and z_{ZAMS} .

In Figure 4 we show the merger rate per comoving volume distribution over redshift/Universe age at merger, for all BCMS, for each z_{ZAMS} . While younger systems naturally merge later, we also see a strong increase in the peak merger rate with z_{ZAMS} and in the overall merger rate with z_{merger} . This indicates that a much greater merger rate in the past is related to a tendency of older populations to produce more BCMS, which could be linked to a top-heavy IMF at large redshift.

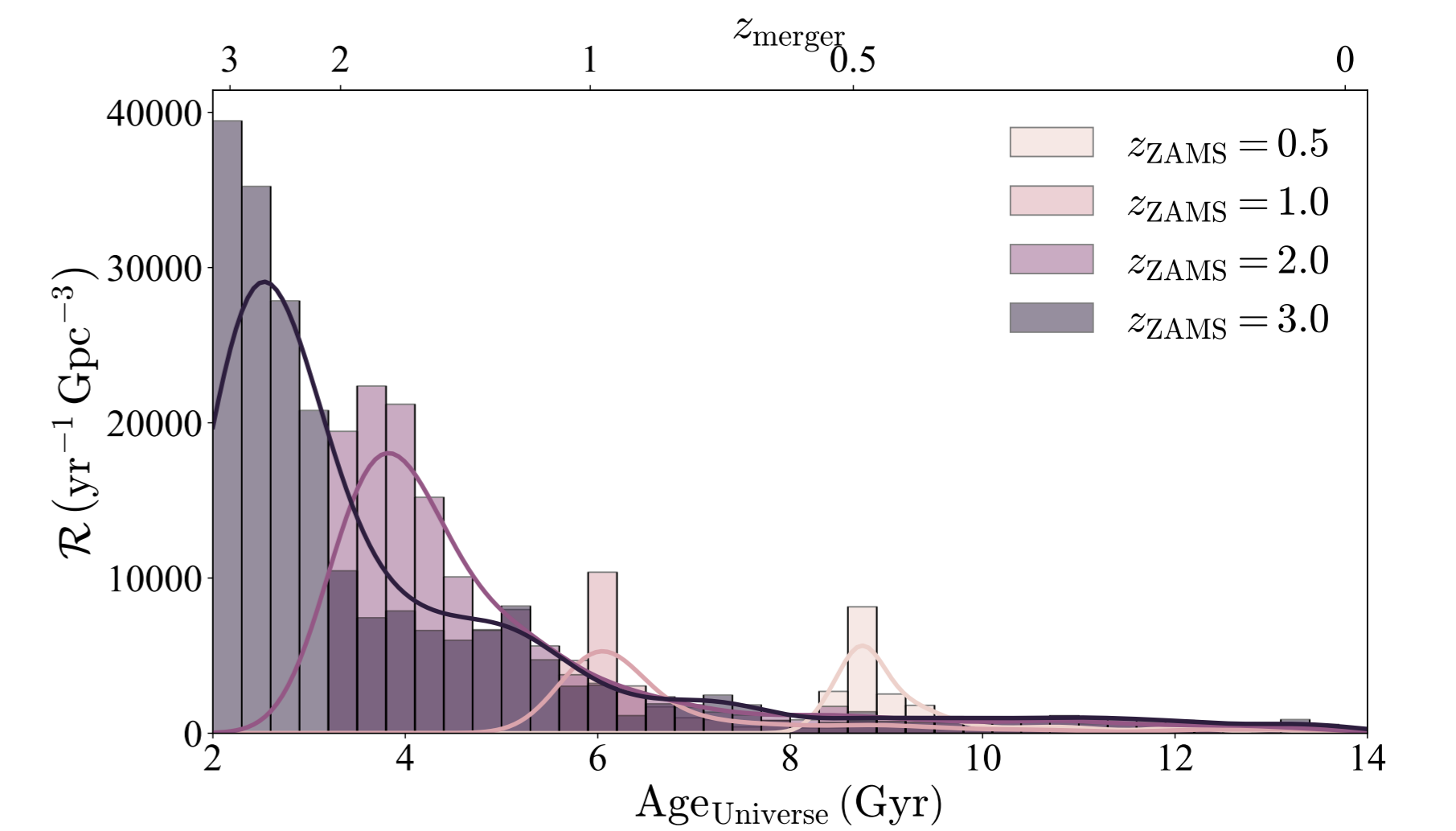


Figure 4: Merger rate distribution for all BCMS over universe age at merger, for each z_{ZAMS} .

We show also the overall binary black hole (BBH) merger rate, \mathcal{R}^{BBH} , distribution with z_{merger} in Figure 5, where a strong preference for massive mergers can be seen with increasing z_{merger} . This behavior suggests that, if observed, such a mass-redshift dependence could be linked to a non-universal IMF. If supported, the IGIMF employed here indicates that the total mass of BCMS could be applied as a good distance proxy.

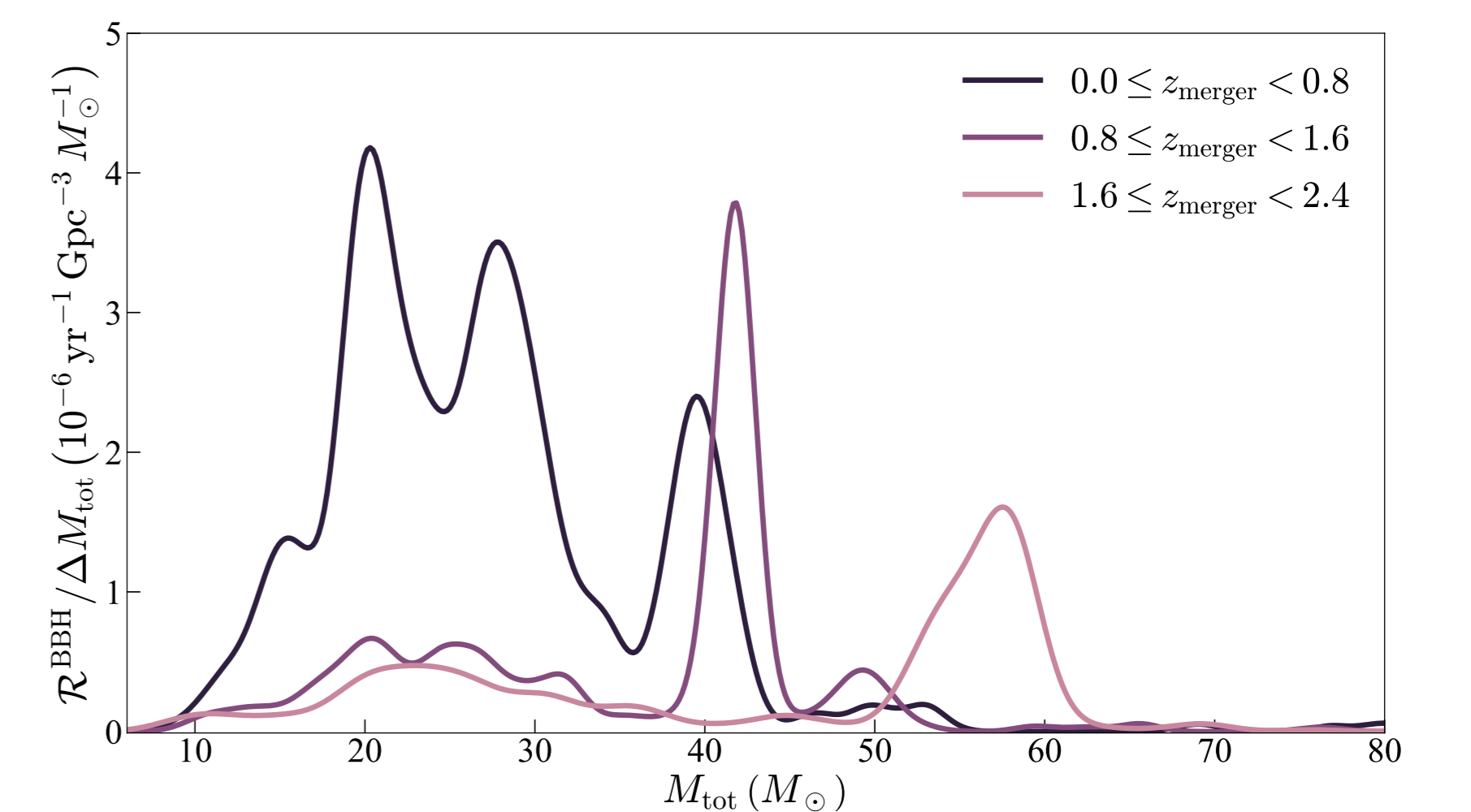


Figure 5: BBH merger rate per total mass bin distribution, for three different z_{merger} ranges.

Finally, we report in Table 1 the approximate merger rates at $z_{\text{merger}} = 0$ from our current sample. We stress that, as our metallicity resolution is still low, these are only preliminary estimates, with the BNS sample in particular being still very limited. That considered, we note that only \mathcal{R}^{BBH} falls outside of the current LIGO 90% credibility interval; if this behavior is kept at higher resolutions, a different metallicity distribution might be favored over our fiducial model.

Source	Local merger rate ($\text{yr}^{-1} \text{Gpc}^{-3}$)		
	BBH	BHNS	BNS
This work	432	124	63
GWTC-3	16 – 130	7.4 – 320	13 – 1900

Table 1: Local merger rates from this work and 90 % credibility intervals from GWTC-3.

Conclusions

In this work we have sought to fully incorporate both a non-universal, cosmically evolving, IGIMF and empirically-fitted correlated binary parameter distributions into the sampling of ZAMS binaries to be evolved with the COMPAS BPS code. By sampling environmental conditions according to the GSMF at different redshift, we have been able to distinguish populations by age and compute time-evolving merger rates. While our sample has not yet achieved the desired resolution we have been able to estimate from it merger rates of 432, 124 and 63 $\text{yr}^{-1} \text{Gpc}^{-3}$ for BBH, BHNS and BNS mergers, the last two of which are compatible with the most recent LIGO estimates. We have also found that an IMF that becomes top-heavy at large redshifts leads to a strong preference of more massive BCMS for higher redshifts. A full exploration of compact binary parameters and evaluation of the effects of the inter-correlated distributions remains to be performed.

References

- Chruślińska M., Jeřábková T., Nelemans G., Yan Z., 2020, A&A, 636, A10
 Jeřábková T., Hasani Zonoozi A., Kroupa P., Beccari G., Yan Z., Vazdekis A., Zhang Z. Y., 2018, A&A, 620, A39
 M. Marks, P. Kroupa, J. Dabringhausen, and M. S. Pawłowski., 2012, MNRAS, 422, 3
 Moe M., Di Stefano R., 2017, ApJS, 230, 15
 Team COMPAS: Riley J., et al., 2022, ApJS, 258, 34

Acknowledgements

Financial support was provided by the Fapesp Agency through the grants 13/26258-4 and 2020/08518-2. LMS acknowledges CNPq for financial support, grant number 140794/2021-2.